

Tank-treading as a means of propulsion in viscous shear flows

By PIERO OLLA^{1,2}

¹ ISAC-CNR, Sez. Cagliari, I-09042 Monserrato, Italy

² INFN, Sez. Cagliari, I-09042 Monserrato, Italy

(Received ?? and in revised form ??)

The use of tank-treading as a means of propulsion for microswimmers in viscous shear flows is taken into exam. We discuss the possibility that a vesicle be able to control the drift in an external shear flow, by varying locally the bending rigidity of its own membrane. By analytical calculation in the quasi-spherical limit, the stationary shape and the orientation of the tank-treading vesicle in the external flow, are determined, working to lowest order in the membrane inhomogeneity. The membrane inhomogeneity acts in the shape evolution equation as an additional force term, that can be used to balance the effect of the hydrodynamic stresses, thus allowing the vesicle to assume shapes and orientations that would otherwise be forbidden. The vesicle shapes and orientations required for migration transverse to the flow, together with the bending rigidity profiles that would lead to such shapes and orientations, are determined. A simple model is presented, in which a vesicle is able to migrate up or down the gradient of a concentration field, by stiffening or softening of its membrane, in response to the variations in the concentration level experienced during tank-treading.

1. Introduction

Microorganisms such as bacteria and protozoa are able to swim in a viscosity dominated environment through a variety of strategies. Some of them, such as amoebae and some bacteria, exploit deformations in their main body (Berg 1976), others utilize cilia (Blake 1971; Blake & Sleight 1974) or flagella (Blum & Hines 1979; Berg 2004), still others, such as cyanobacteria, are able to generate travelling waves on their surface (Ehlers *et Al.* 1996). In all cases, contrary to what happens at macroscopic scales, fluid inertia plays no role, and microscopic swimming is essentially a low Reynolds number affair (Lighthill 1957; Childress 1981) (see Lauga & Powers (2009) for a recent review).

One of the motivations for the interest in swimming at low Reynolds numbers is its relevance for the future realization of artificial microswimmers, which would have widespread applications in medicine and in the industry. Over the years, various propulsion schemes have been proposed, both discrete (typically, an assembly of rigid parts hinged together, or connected through immaterial links and springs; see e.g. Purcell (1977); Najafi & Golestanian (2004); Avron *et Al.* (2005)) and continuous (Lighthill 1952; Stone & Samuel 1996; Ishikawa & Pedley 2008). In all cases, proper design of a microswimmer entails a complex optimization problem, which must take into account limitations, such as those imposed by the scallop theorem (Purcell 1977; Shapere & Wilczek 1989).

Recently, progress in mechanical manipulation at the microscale has allowed to realize the first examples of artificial microscopic swimmers (Dreyfus *et Al.* 2005; Yu *et Al.*

2006; Behkam & Sitti 2006; Tierno *et Al.* 2008; Leoni *et Al.* 2009). At the present stage, however, most of such artificial swimmers are driven by external fields and the problem of an autonomous power source remains under study. Among the solutions that have been taken into consideration, various methods of rectification of Brownian motion (Lobaskin *et Al.* 2008; Golestanian & Ajdari 2009), and mechanical reactions in the swimmer body, induced by inhomogeneity in the environment, e.g. a chemical gradient (Golestanian *et Al.* 2005; Paxton *et Al.* 2006; Pooley & Balazs 2007).

Given the fact that a microswimmer typically lives in a non-quiescent environment, a possibility that has been taken into consideration, is to exploit the velocity fields already present in the fluid as an energy source for propulsion. Such a swimmer would sail through the fluid, by a sequence of deformations induced in its body by the hydrodynamic stresses in the external flow. A recent example of such “passive” swimming has been illustrated in Olla (2010), based on a discrete swimmer design similar to the one considered in Najafi & Golestanian (2004) and Golestanian & Adjari (2008).

It should be mentioned that passive swimming (at microscopic scales) already exists in nature. An example is the Fahraeus-Lindqvist effect (Vand 1948): a red cell in a small artery will deform in response to the flow, in such a way to be pushed to the vessel center, thus decreasing its fluid-mechanic resistivity. In analogous way, vesicles are able to migrate transverse to a wall bounded shear flow thanks to tank-treading (Olla 1997; Sukumaran & Seifert 2001; Abkarian *et Al.* 2002), and similar behavior have been observed in quadratic shear flows as well (Olla 2000; Coupier *et Al.* 2008; Danker *et Al.* 2009).

Tank-treading has already been taken into consideration as a possible microswimmer propulsion system (Purcell 1977; Lehsansky & Kenneth 2008) (see also Tierno *et Al.* (2008) for a somehow related approach). It is not too much of a surprise, therefore, that the optimal strategy for a passive discrete microswimmer in a viscous flow turns out to be a discrete version of tank-treading (Olla 2010). It is natural to ask what would be an appropriate design for a continuous counterpart of this device. We shall concentrate our analysis on continuous microswimmers whose basic structure is that of a vesicle.

One of the motivations for the present study is that the efficiency of a discrete swimmer, of the kind considered in Najafi & Golestanian (2004) and Golestanian & Adjari (2008), is rather low. It is in fact $\propto a\delta R/R^2$, where a the size of the moving parts, δR is the stroke amplitude, R is the body size; typically: $a/R, \delta R/R \ll 1$. In the case of a continuous swimmer, instead, $a/R \equiv 1$ and the efficiency would become $\propto \delta R/R$.

The complicated problem lies in the design of an appropriate control system for such a device. In the absence of a control system, a simple vesicle, immersed in a linear shear flow, will stay naturally in a tank-treading condition, provided the viscosity contrast between interior and exterior fluid is not too high (Kraus *et Al.* 1996). A sketch of a tank-treading vesicle in a linear shear is provided in Fig. 1. Tank-treading will make such a vesicle migrate away from a solid wall perpendicular to the shear plane and parallel to the flow, but, unfortunately, no other migration behaviors are possible. Migration towards a wall, for example, would require an impossible condition, in which, the tank-treading vesicle maintains an ellipsoidal shape, with long axis aligned with the contracting direction of the strain component of the shear. For similar reasons, no transverse migration would be possible in an unbounded shear flow. The missing ingredient is some mechanism to generate internal stresses that counteract the straining action of the external flow.

We want to explore the possibility that a vesicle be able to generate such stresses through appropriate modification of its membrane properties, namely, local stiffening or softening of its outer surface. (We hypothesize that the energy required for stiffening and softening of the membrane be negligible compared to the one that would expended to

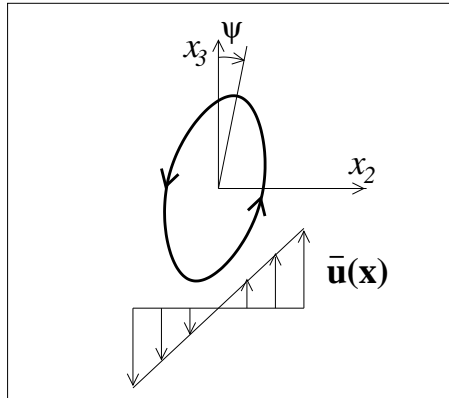


FIGURE 1. Tank-treading vesicle in a linear shear: the membrane circulates around the vesicle interior preserving the shape and orientation of the object. A vesicle with a homogeneous membrane will maintain an overall ellipsoidal shape, with long axis at an angle $\psi < \pi/4$ with respect to the direction of the flow. Low internal viscosities correspond to $\psi \simeq \pi/4$; high internal viscosities will lead to $\psi \rightarrow 0$ and then to transition to regimes in which the vesicle rotates more or less as a rigid object.

achieve an identical migration velocity without the help of the external flow; in this sense, we speak of a passive swimmer. Although natural at the macroscale, this hypothesis may require further justification in the case of microscopic objects). Notice that the presence of a mere inhomogeneity in the membrane, say an inclusion, would be insufficient to this goal. Such an inhomogeneity would be advected by the membrane flow and would be unable to lead to a stationary vesicle configuration. The inhomogeneity of the membrane must not vary with time in a laboratory reference frame, which implies that the membrane elements must continuously change their properties, as they tank-tread around the vesicle.

The mechanism through which local modifications of the membrane stiffness lead to the generation of stresses in the fluid, closely resembles the one responsible for the Marangoni effect (Young *et Al.* 1959; Subramanian & Balasubramaniam 2001). Marangoni effects have been considered indeed as a possible mechanism of self-propulsion for droplets in inhomogeneous environments (Kitahata *et Al.* 2002; Furtado *et Al.* 2008), and Hanna & Vlahovska (2010) have studied the Marangoni stresses, generated by an external shear induced redistribution of a surfactant over a droplet.

The philosophy in the present paper is different: the membrane stresses do not act directly, through internal flows in the vesicle, to generate propulsion; they rather contribute to modify the vesicle shape, and propulsion is achieved through interaction between a fixed non-spherical shape and the external flow.

We shall consider the case of an ideal membrane, so that the only material property that must be taken into account is a bending rigidity. The specific behavior we shall be interested in is the transverse drift in an unbounded linear shear, already considered in Olla (2010). We shall determine the bending rigidity profile that would generate such behavior, and investigate the possibility that the required bending rigidity profiles be obtained as a direct response of the membrane to the external environment, without the need of an “intelligent”, internal control system.

An analytical treatment of the problem is possible only in the case of quasi-spherical vesicles, and, for this purpose, the analysis in Seifert (1999) and Olla (2000) will be generalized to the case of an inhomogeneous membrane. As discussed in Farutin *et Al.*

(2010), the perturbative problem is singular and care must be taken to scale appropriately the shear strength and the viscosity contrast between inner and outer fluid, in function of the deviation from spherical shape of the vesicle. For the sake of simplicity, contrary to Seifert (1999), all finite temperature effect, will be disregarded in the analysis.

This paper is organized as follows. In Sec. 2 the bending forces exerted on the ambient fluid by a quasi-spherical inextensible membrane, will be calculated, generalizing to the case of an inhomogeneous bending rigidity, the analysis in Zhong-can & Helfrich (1989). In Sec. 3, the shape dynamics of a vesicle with an inhomogeneous membrane, in a viscous shear flow, will be analyzed. In Sec. 4, the possibility of drift of a tank-treading vesicle in an unbounded shear flow will be discussed, and the bending rigidity profiles required for drift will be determined. In Sec. 5, a simple model of vesicle, with a membrane that changes properties in response to the external environment, will be presented, and the migration behavior of the vesicle will be discussed. Section 6 is devoted to conclusions. Additional technical details will be presented in the Appendices.

2. The inhomogeneous membrane

The shape of a vesicle can be described in terms of the position $\mathbf{R}(s_1, s_2)$ of the points on the membrane, in function of a suitable set of curvilinear coordinates $s_{1,2}$. For a quasi-spherical vesicle, it is natural to work in spherical coordinates r, θ, ϕ , such that $\mathbf{R} = R(\theta, \phi)\mathbf{e}_r$, and we write

$$R(\theta, \phi) = R_0[1 + \tilde{R}(\theta, \phi)], \quad (2.1)$$

where R_0 is the radius of the sphere with volume equal to that of the vesicle.

We can decompose the scalar field \tilde{R} in spherical harmonics: $\tilde{R}(\theta, \phi) = \sum_{lm} \tilde{R}_{lm} \times Y_{lm}(\theta, \phi)$. In analogous way, vector fields, such as e.g. the displacement $\delta\mathbf{R}(\theta, \phi)$ of a membrane point initially at $\mathbf{R}(\theta, \phi)$, will be expanded on the vector spherical harmonics basis:

$$\mathbf{Y}_{Slm} = Y_{lm}\mathbf{e}_r, \quad \mathbf{Y}_{Elm} = \frac{r\nabla Y_{lm}}{\sqrt{l(l+1)}}, \quad \mathbf{Y}_{Mlm} = \mathbf{e}_r \times \mathbf{Y}_{Elm}, \quad (2.2)$$

so that $\delta\mathbf{R} = \sum_{\mu lm} \delta R_{\mu lm} \mathbf{Y}_{\mu lm}$. The basis in (2.2) can easily be verified to be orthonormal: $\langle \mu lm | \mu' l' m' \rangle \equiv \int \mathbf{Y}_{\mu lm}^* \cdot \mathbf{Y}_{\mu' l' m'} \sin\theta d\theta d\phi = \delta_{\mu\mu'} \delta_{ll'} \delta_{mm'}$.

Assuming that the vesicle has volume $V = \frac{4}{3}\pi R_0^3$, it is possible to express the vesicle area in terms of the components \tilde{R}_{lm} through the formula:

$$S = (4\pi + \epsilon)R_0^2, \quad \epsilon = \frac{1}{2} \sum'_{lm} (l^2 + l - 2) |\tilde{R}_{lm}|^2 + O(\tilde{R}^3), \quad (2.3)$$

where $\sum'_{lm} \equiv \sum_{l \geq 2} \sum_{m=-l}^l$ (Seifert 1999). The excess area $\epsilon \ll 1$ in Eq. (2.3), which parameterizes the deviation from spherical shape, will serve as an expansion parameter for the theory. Notice that the $l = 1$ terms in the sum in Eq. (2.3) are identically zero, which reflects the fact, that the components $\tilde{R}_{l=1,m}$, to lowest order in ϵ , correspond to a rigid displacement of the vesicle.

Following Zhong-can & Helfrich (1989), the bending energy of an inhomogeneous membrane can be expressed as surface integral

$$\mathcal{H}^B = \frac{1}{2} \int \kappa (2H - C)^2 dS, \quad (2.4)$$

where H is the mean curvature of the membrane, which can be written in the form

(Zhong-can & Helfrich 1989): $H = \frac{1}{2}\mathbf{n} \cdot \nabla_{\mathbf{t}}^2 \mathbf{R}$, with \mathbf{n} is the unit normal and $\nabla_{\mathbf{t}}^2$ the Laplace-Beltrami operator on the membrane; C is called the spontaneous curvature, and κ is the bending rigidity. For the sake of simplicity, we shall assume symmetry of the membrane, and set $C = 0$. Following Jenkins (1977), to enforce inextensibility of the membrane, we include a position dependent surface tension in the energy integral

$$\mathcal{H}^B \rightarrow \mathcal{H} = \mathcal{H}^B + \kappa_0 \int T dS, \quad (2.5)$$

where T plays the role of a Lagrange multiplier coupled to the local area element dS .

Let us suppose the membrane is able to react to the external environment through local variations of its bending rigidity:

$$\kappa = \kappa_0 [1 + \tilde{\kappa}(\mathbf{R}, t)], \quad (2.6)$$

where, as in Goulian *et Al.* (1993), $\tilde{\kappa}$ is assumed small and will serve, together with ϵ , as a basis for a perturbation expansion in Eqs. (2.4). For the moment, we assume the profile $\tilde{\kappa}(\mathbf{R}, t)$ to be assigned, and postpone to Sec. 5 any consideration on the dynamical mechanisms determining its form.

The membrane will act on the fluid with a force density

$$\mathbf{f}(\mathbf{r}, t) = - \int \frac{\delta \mathcal{H}}{\delta \mathbf{R}(\theta, \phi)} \delta(\mathbf{r} - \mathbf{R}(\theta, \phi)) d\theta d\phi, \quad (2.7)$$

which will be the sum of a bending force \mathbf{f}^B and a tension force \mathbf{f}^T . In the case of a homogeneous membrane, the bending force would be directed along the normal to the membrane. The space dependence of κ produces a tangential force component. In fact, the variation of bending energy produced by a deformation field $\delta \mathbf{R}(\theta, \phi)$ can be written in the form

$$\delta \mathcal{H}^B = \delta \mathcal{H}^B = \int \delta \mathbf{R} \cdot \left[\frac{\delta \mathcal{H}^B}{\delta \mathbf{R}_{\mathbf{n}}} - 2JH^2 \nabla_{\mathbf{t}} \kappa \right] d\theta d\phi. \quad (2.8)$$

where $Jd\theta d\phi = dS$ is the surface element of the undeformed membrane, and subscripts \mathbf{n} and \mathbf{t} identify normal and tangential vector components. The tangential contribution in Eq. (2.8) accounts for the variation of bending rigidity at position \mathbf{R} , from tangential displacement of a membrane element from position $\mathbf{R} - \delta \mathbf{R}_{\mathbf{t}}$ to \mathbf{R} .

To lowest order in ϵ , $\delta \mathbf{R}_{\mathbf{t}}$ is a combination of vector harmonics $\mathbf{Y}_{\mu l m}$ with $\mu = E, M$. From the relation $\int \mathbf{Y}_{M l m} \cdot \nabla Y_{l' m'} dS = 0$ [see Eq. (2.2)], the tangential component of Eq. (2.8) has only components from $\delta R_{E l m}$. As it will soon become clear [see Eq. (3.9) below], this implies that flows on the membrane, induced by inhomogeneity of κ , are necessarily associated with vesicle deformations.

To explicitly calculate the bending force, we expand the mean curvature H and the Jacobian in powers of ϵ . The mean curvature of a quasi-spherical membrane was calculated in Zhong-can & Helfrich (1989), and can be rewritten in the form:

$$H = \frac{1}{R_0} [-1 + (1 + \frac{1}{2} \tilde{\nabla}_{\mathbf{t}}^2) \tilde{R} - \tilde{R} (1 + \tilde{\nabla}_{\mathbf{t}}^2) \tilde{R} + O(\epsilon^{3/2})], \quad (2.9)$$

where $\tilde{\nabla}_{\mathbf{t}} \equiv R_0 \nabla_{\mathbf{t}}$. In analogous way, we can write for the Jacobian:

$$J = R_0^2 \sin \theta \left[(1 + \tilde{R})^2 + \frac{1}{2} \left((\partial_{\theta} \tilde{R})^2 + \frac{(\partial_{\phi} \tilde{R})^2}{\sin^2 \theta} \right) + O(\epsilon^{3/2}) \right]. \quad (2.10)$$

Substituting into Eq. (2.4), we obtain the expression for the bending energy: $\mathcal{H}^B = \kappa_0 \int \{ 2 + 2\tilde{\kappa} [1 - \tilde{\nabla}_{\mathbf{t}}^2 \tilde{R}] + \tilde{R} \tilde{\nabla}_{\mathbf{t}}^2 \tilde{R} + \frac{1}{2} (\tilde{\nabla}_{\mathbf{t}}^2 \tilde{R})^2 + O(\epsilon^{3/2}) + O(\tilde{\kappa} \epsilon) \} \sin \theta d\theta d\phi$. Exploiting Eqs.

(2.8) and (2.7), using the expression $\tilde{\nabla}_{\mathbf{t}}^2 = \partial_{\theta}^2 + \cot \theta \partial_{\theta} + (\sin \theta)^{-2} \partial_{\phi}^2 + O(\epsilon^{1/2})$, and expanding on the basis (2.2), we obtain the following expression for the bending force density, valid to lowest order in ϵ and $\tilde{\kappa}$:

$$\begin{aligned} \mathbf{f}^B = & -\frac{\kappa_0}{R_0^3} \sum_{lm} \{l(l+1)[(l^2+l-2)\tilde{R}_{lm} + 2\tilde{\kappa}_{lm}]\mathbf{Y}_{Slm} \\ & - 2\sqrt{l(l+1)}\tilde{\kappa}_{lm}\mathbf{Y}_{Elm}\} \delta(r-R_0). \end{aligned} \quad (2.11)$$

To this order of accuracy, the bending force acts on the fluid at the spherical surface $r = R_0$. Taking for $\tilde{\kappa}_{lm}$, the spectrum produced by a discrete set of inhomogeneities (e.g. inclusions) in the membrane, Eq. (2.11) would lead to the zero temperature expressions for the interaction forces among such inhomogeneities, calculated in Goulian *et Al.* (1993). Notice that inhomogeneity of the membrane produces a tangential component in the bending force, that, in order for membrane area to be conserved, must be counter-balanced by tension forces.

The tension force \mathbf{f}^T is obtained from variation of $\int T J d\theta d\phi$. We restrict our analysis to a situation in which $T = O(\epsilon^{1/2})$, corresponding to a weak shear regime in which the hydrodynamic and the bending stresses, that must be balanced by \mathbf{f}^T , are of the same order [see Eq. (3.6) below]. Global area changes are quadratic in \tilde{R} , while local changes are linear, hence, it is convenient to separate in the tension, global and local contributions: $T = T^{glo} + T^{loc}$. The variation of the anisotropic part is $\int T^{loc} \delta J d\theta d\phi = \int \delta \mathbf{R} \cdot [2(T^{loc}/R_0)\mathbf{e}_r - \nabla_{\mathbf{t}} T^{loc} + O(\epsilon)] J d\theta d\phi$. This leads to the contribution to the tension force, to lowest order in ϵ : $\mathbf{f}^{T,loc} = -(\kappa_0/R_0^3)[2(T^{loc}/R_0)\mathbf{e}_r - \nabla_{\mathbf{t}} T^{loc}] \delta(r-R_0)$.

The isotropic contribution to the tension energy is $\kappa_0 T^{glo} S$; its variation is simply $\kappa_0 T^{glo} \delta S$, which, from Eq. (2.3) leads immediately to the result, expanding in vectors spherical harmonics: $\mathbf{f}^{T,glo} = -(\kappa_0 T^{glo}/R_0^3) \sum_{lm} (l^2+l-2)\tilde{R}_{lm} \mathbf{Y}_{Slm} \delta(r-R_0)$ (Seifert 1999). Expanding also $\mathbf{f}^{T,loc}$ in vector spherical harmonics, and summing to $\mathbf{f}^{T,glo}$, we obtain

$$\begin{aligned} \mathbf{f}^T \equiv \mathbf{f}^{T,glo} + \mathbf{f}^{T,loc} = & -\frac{\kappa_0}{R_0^3} \sum_{lm} \{[(l^2+l-2)T^{glo}\tilde{R}_{lm} + 2T_{lm}^{loc}]\mathbf{Y}_{Slm} \\ & - \sqrt{l(l+1)}T_{lm}^{loc}\mathbf{Y}_{Elm}\} \delta(r-R_0). \end{aligned} \quad (2.12)$$

Setting $\mathbf{f}_{\mathbf{t}}^B + \mathbf{f}_{\mathbf{t}}^T = 0$, we obtain the local tension T_{lm}^{loc} in the absence of external flow. Substituting into the normal component $\mathbf{f}_{\mathbf{n}}^T$, it is possible to see that the contribution by inhomogeneity of the membrane, to the total normal force $\mathbf{f}_{\mathbf{n}} = \mathbf{f}_{\mathbf{n}}^B + \mathbf{f}_{\mathbf{n}}^T$, is $\mathbf{f}_{\mathbf{n}}^{in} = -\frac{2\kappa_0}{R_0^3} \sum_{lm} (l^2+l-2)\tilde{\kappa}_{lm} \mathbf{Y}_{Slm}$ (we shall identify contributions by inhomogeneity of the membrane, in general, with superscript “*in*”). As it could be expected from analogous behavior in the case of a homogeneous membrane, the $l = 1$ components of \mathbf{f}^{in} , associated with rigid displacement of the vesicle, do not contribute to the sum. Notice however that the $l = 1$ components of \mathbf{f}^B and \mathbf{f}^T do not balance in general, and a vesicle with an inhomogeneous, arbitrarily compressible membrane, could propel itself in a quiescent fluid through a mechanism analogous to the Marangoni effect. A combination of inhomogeneous bending rigidity and surface tension, rather than just an inhomogeneous surface tension (see e.g. Kitahata *et Al.* (2002)), would be responsible in this case for propulsion. More precisely, it is f_{S1m} that is directly responsible for propulsion (we recall that the induced deformation components δR_{S1m} , to lowest order in ϵ , describe rigid displacements), while f_{E1m} can be shown to generate flows inside the vesicle, analogous to the convection-like rolls that are present in a droplet experiencing Marangoni propulsion.

3. Deformations in an external shear flow

We want to determine the shape evolution equation for a vesicle with inhomogeneous membrane, immersed in the shear flow

$$\bar{\mathbf{u}}(\mathbf{x}, t) = \alpha x_2 \hat{\mathbf{x}}_3 \quad (3.1)$$

($x_1 = r \sin \theta \cos \phi$, $x_2 = r \sin \theta \sin \phi$ and $x_3 = r \cos \theta$). The derivation closely follows the one in Seifert (1999), with additional care, in light of the results in Farutin *et Al.* (2010), given to the singular behaviors taking place in the limit $\tilde{\kappa}, \epsilon \rightarrow 0$. Identifying with η_{in} and η_{out} the dynamical viscosities of the fluid inside and outside the vesicle, we can introduce dimensionless constants, the capillary number Ca and the viscosity contrast λ :

$$\text{Ca} = \frac{\eta_{out} \alpha R_0^3}{\kappa_0} \quad \text{and} \quad \lambda = \frac{\eta_{in}}{\eta_{out}}, \quad (3.2)$$

parameterizing the relative importance of hydrodynamic forces to internal membrane stresses, and the ratio between internal and external fluid viscosities.

The vesicle will produce a flow perturbation $\hat{\mathbf{u}}$ to be added to $\bar{\mathbf{u}}$ on the outside of the vesicle, and a flow field \mathbf{u} inside the vesicle. The boundary condition at the membrane will thus read $\bar{\mathbf{u}}(\mathbf{R}, t) + \hat{\mathbf{u}}(\mathbf{R}, t) = \mathbf{u}(\mathbf{R}, t)$, and to this we must add the boundary conditions $\hat{\mathbf{u}} = 0$ at $r \rightarrow \infty$ and $\mathbf{u} = 0$ at $x = 0$. Let us indicate with capital letters values of the fluid velocity on the membrane. Expanding in the basis of Eq. (2.2), the boundary condition on the membrane becomes:

$$U_{\mu lm} = \bar{U}_{\mu lm} + \hat{U}_{\mu lm}. \quad (3.3)$$

In creeping flow conditions, the viscous forces by the fluid are balanced by the reaction force exerted by the membrane. To lowest order in ϵ , the force balance at the vesicle surface, is evaluated at $r = R_0$, and the boundary condition equation (3.3) is enforced at $r = R_0$ as well. To this order in ϵ , from membrane inextensibility, such boundary conditions are the ones imposed on the fluid by a rigid spherical surface:

$$\begin{aligned} \hat{u}_{\mu lm}^{(0)}(R_0) &\equiv \hat{U}_{\mu lm}^{(0)} = -\bar{U}_{\mu lm}^{(0)} \equiv -\bar{u}_{\mu lm}^{(0)}(R_0), & \mu = \text{S, E}; \\ u_{\mu lm}^{(0)}(R_0) &\equiv U_{\mu lm}^{(0)} = \bar{U}_{\mu lm}^{(0)} \equiv \bar{u}_{\mu lm}^{(0)}(R_0), & \mu = \text{M}, \end{aligned} \quad (3.4)$$

where superscripts indicate order in $\epsilon^{1/2}$. In the following, although $\tilde{\kappa}$ and \tilde{R} (or $\epsilon^{1/2}$) are not in general quantities of the same order of magnitude, we shall use superscripts to indicate simultaneously order in $\tilde{\kappa}$ and $\epsilon^{1/2}$ [for instance, what we have calculated in Eq. (2.11) is actually $\mathbf{f}^{B,(1)}$].

We see that $U_{Slm}^{(0)} = U_{Elm}^{(0)} = \hat{U}_{Mlm}^{(0)} = 0$. (Besides, it is possible to see that absence of external torques implies $\hat{u}_{M1m} = 0$ to all order in \tilde{R}).

To lowest order in ϵ , the force balance equation will take the form:

$$f_{\mu lm} + \alpha \eta_{out} [\hat{g}_{\mu lm}(\hat{\mathbf{U}}^{(0)}) - g_{\mu lm}(\bar{\mathbf{U}}^{(0)}) + \lambda g_{\mu lm}(\mathbf{U}^{(1)})] \delta(r - R_0) = 0, \quad (3.5)$$

where $\hat{\mathbf{g}}$ and \mathbf{g} indicate components of the adimensionalized hydrodynamic surface force density, associated with fluid flow components vanishing, respectively, at $r \rightarrow \infty$ and $r \rightarrow 0$ (notice that g is defined as as the force density exerted by a flow inside the membrane, whence the minus sign in front of the contribution by $\bar{\mathbf{U}}^{(0)}$; see Appendix A). Inspection of Eqs. (2.11, A 5-A 6) shows us that, in order for all the terms in Eq. (3.5) to be of the same order of magnitude, the dimensionless parameters Ca and λ must satisfy:

$$\text{Ca} = O(\epsilon^{1/2}) \quad \text{and} \quad \lambda = O(\epsilon^{-1/2}), \quad (3.6)$$

corresponding to a regime of weak shear and strong viscosity contrast.

The velocity field \mathbf{U} determines the membrane dynamics. In particular, the membrane displacement rate $\dot{R}(\theta, \phi; t)$ obeys the equation (Seifert 1999):

$$\dot{R} = U_r + \mathbf{U} \cdot \nabla_{\mathbf{t}} R. \quad (3.7)$$

From Eq. (3.4) [see also Eq. (A 4)], $\mathbf{U}^{(0)}$ is purely due to the vorticity component of $\bar{\mathbf{u}}$, hence, to lowest order in \dot{R} : $R^{(1)} = U_r^{(1)} + \bar{\mathbf{u}}_{r=R_0}^{rot} \cdot \nabla_{\mathbf{t}} R$, where $\bar{\mathbf{u}}^{rot} = \frac{1}{2}\alpha(x_2\hat{\mathbf{x}}_3 - x_3\hat{\mathbf{x}}_2)$, that is the vorticity part of the shear flow $\bar{\mathbf{u}}$. The advection term in Eq. (3.7) can then be eliminated working in a reference frame rotating with the vorticity of the flow. We thus have, for the $\mu = S$ component of $\mathbf{U}^{(1)}$ needed in $g_{\mu lm}^{(0)}(\mathbf{U}^{(1)})$:

$$U_{Slm}^{r,(1)} = \dot{R}_{lm}^r, \quad (3.8)$$

and we have introduced a superscript r as a reminder that the components are calculated in the rotating reference frame.

It is possible to see that local inextensibility leads to the following relation between velocity components on the membrane (Seifert 1999; Olla 2000):

$$U_{Elm}^{(1)} = \frac{2}{\sqrt{l(l+1)}} U_{Slm}^{(1)}. \quad (3.9)$$

Working in the rotating reference frame, Eq. (3.9) can then be used, together with Eq. (3.8), to express the components \mathbf{U}_{Elm} in Eq. (3.5) in function of \dot{R}_{lm} .

The $\mu = E$ component of Eq. (3.5) can be used at this point to express the local tension T_{lm}^{loc} in function of the tangential components of \mathbf{f}^B and of the hydrodynamic force. Substituting into the $\mu = S$ component of Eq. (3.5) and using Eq. (3.4) to express $\hat{\mathbf{U}}$ in function of $\bar{\mathbf{U}}$, we remain with a first order differential equation for the deformation component \tilde{R}_{lm} . Using Eqs. (2.11-2.12), and (A 5-A 6) to explicitate the various force contributions, we obtain the equation for the deformation dynamics in the rotating reference frame:

$$\lambda \text{Ca} A_l \frac{d\tilde{R}_{lm}^r}{d\tilde{t}} + B_l \tilde{R}_{lm}^r = \text{Ca} C_{lm}^r + D_l \tilde{\kappa}_{lm}^r, \quad (3.10)$$

where $\tilde{t} = \alpha t$,

$$\begin{aligned} A_l &= \frac{2l^3 + 3l^2 - 5}{l(l+1)}, & B_l &= (l^2 + l - 2)[l(l+1) + T^{glo}], \\ C_{lm}^r &= \frac{1}{R_0\alpha} \left[\frac{4l^3 + 6l^2 - 4l - 3}{l(l+1)} \bar{U}_{Slm}^r + \frac{2l+1}{\sqrt{l(l+1)}} \bar{U}_{Elm}^r \right], \\ D_l &= -2(l^2 + l - 2). \end{aligned} \quad (3.11)$$

and the global tension T^{glo} is determined from the constrain equation (2.3). That all the terms in Eq. (3.10) contribute to the same order in ϵ becomes particularly important at the cross-over line in the Ca, λ , where the tank-treading regime [the stationary solution to Eq. (3.10)] is only marginally stable. As discussed in Farutin *et Al.* (2010), analysis of the crossover region for generic Ca would require inclusion of all $O(\epsilon)$ terms in Eq. (3.10). The choice $\text{Ca} = O(\epsilon^{1/2})$ allows us to circumvent such difficulties.

For $\tilde{\kappa} = 0$, these equations correspond to the ones obtained in Seifert (1999) and Olla (2000). They differ only for the expression of the coefficient of the time derivative, that, to the order considered in ϵ , due to the ordering in Eq. (3.6), must contain only terms linear in λ .

In order to return to the laboratory frame, it is sufficient to include in the time deriva-

tive in Eq. (3.10) the effect of rotation:

$$\frac{d\tilde{R}_{lm}^r}{dt} \rightarrow \frac{d\tilde{R}_{lm}}{dt} + \sum_{m'} \Omega_{lmm'} \tilde{R}_{lm'}, \quad (3.12)$$

where $\Omega_{lmm'} = 0$ unless $m' = m \pm 1$, in which case:

$$\Omega_{l,m,m-1} = \Omega_{l,m-1,m} = \frac{i}{4} \sqrt{(l-m+1)(l+m)}. \quad (3.13)$$

Equation (3.10) takes then the form in the laboratory frame:

$$\lambda \text{Ca} A_l \left[\frac{d\tilde{R}_{lm}}{dt} + \sum_{m'} \Omega_{lmm'} \tilde{R}_{lm'} \right] + B_l \tilde{R}_{lm} = \text{Ca} C_{lm} + D_l \tilde{\kappa}_{lm}, \quad (3.14)$$

where now, from Eq. (A 4):

$$C_{lm} = 2i \sqrt{\frac{10\pi}{3}} \delta_{l2} \delta_{|m|1}. \quad (3.15)$$

From Eqs. (3.10) and (3.14), we see that inhomogeneity of the membrane acts in the dynamics as a forcing, which acts side by side with the effect of the external flow. Choosing components $\tilde{\kappa}_{lm}$ appropriately, a tank-treading vesicle in an external shear flow could be stabilized at orientations otherwise impossible to achieve (e.g. an ellipsoidal shape with long axis along the contracting, rather than the expanding strain direction).

4. Drift behaviors

Through tank-treading, a vesicle will be able to maintain a fixed shape and orientation in a stationary external flow. In the absence of inhomogeneities in the membrane, a tank-treading vesicle in the shear flow described by Eq. (3.1), will maintain an ellipsoidal shape with long axis somewhere between the stretching direction of the strain and the flow direction x_3 (Kraus *et Al.* 1996). A fixed orientation is the main ingredient allowing migration of a tank-treading vesicle across the velocity lines of the shear flow, and a vesicle, in the condition described above, would migrate away from a solid plane wall perpendicular to the x_2 axis.

Non-homogeneity of the membrane provides an additional mechanism to control the shape and orientation of a vesicle in an external flow, and could be used in principle to generate drift behaviors that would otherwise be impossible. We shall focus on the problem of generating a transverse drift in the flow of Eq. (3.1), in the case of an unbounded domain.

In order for such a drift to be present, it is necessary that the velocity perturbation $\hat{\mathbf{u}}$ has components $\mu = \text{S, E}$, $l = 1$, signaling the presence of a net hydrodynamic force acting on the vesicle (see Appendix A). To obtain such harmonics, we must include in the boundary condition Eq. (3.3) determining $\hat{\mathbf{u}}$, the effect of non-sphericity of the surface $r = R(\theta, \phi)$. The procedure parallels the one in Olla (2000). To $O(\epsilon^{1/2})$, we can write:

$$\hat{\mathbf{U}}^{(1)} = -(R - R_0) \frac{\partial}{\partial r} (\bar{\mathbf{u}} + \hat{\mathbf{u}}^{(0)})_{r=R_0} + \mathbf{U}^{(1)}, \quad (4.1)$$

from which we get the boundary condition $\hat{\mathbf{u}}_{r=R_0}^{(1)} = \hat{\mathbf{U}}^{(1)}$.

Passing to vector spherical harmonics, Eq. (4.1) will take the form:

$$\hat{U}_{\mu lm}^{(1)} = - \sum_{\mu' l' m'} \langle \mu l m | R | \mu' l' m' \rangle U'_{\mu' l' m'} + U_{\mu lm}^{(1)}, \quad (4.2)$$

where $\mathbf{U}' \equiv \frac{\partial}{\partial r}(\bar{\mathbf{u}}^{(0)} + \hat{\mathbf{u}}^{(0)})_{r=R_0}$. Exploiting Eqs. (A 2-A 4) and (3.4), we can write:

$$U'_{Slm} = 0; \quad U'_{Elm} = \frac{2l+1}{R_0} \left(\frac{-3\bar{U}'_{Slm}}{\sqrt{l(l+1)}} + 2\bar{U}'_{Elm} \right) = i\sqrt{5\pi}\alpha\delta_{l2}\delta_{|m|1}. \quad (4.3)$$

It is possible to see that the contribution to drift from $U_{\mu lm}^{(1)}$ vanishes identically. In fact, in the rotating reference frame, the components $U_{\mu lm}^{(1)}$, $\mu = S, E$ are related to \dot{R}_{lm} through Eqs. (3.8) and (3.9). From Eq. (3.12), we find in the laboratory frame:

$$U_{Elm}^{(1)} = \frac{2}{\sqrt{l(l+1)}} U_{Slm}^{(1)} = \frac{2}{\sqrt{l(l+1)}} \left(\dot{R}_{lm} + \sum_{m'} \Omega_{lmm'} R_{lm'} \right),$$

and we see immediately that $U_{\mu lm}^{(1)} = 0$ for $\mu = S, E$; $l = 1$.

Returning to Eq. (4.2), we see from Eqs. (4.3) and (A 7) that the only surviving terms in the sum are those for $\mu = \mu' = E$, $l = m = 1$ and $l' = 2$, $m' = \pm 1$. Expanding $\langle \mu lm | R | \mu' l' m' \rangle = \sum_{l'' m''} \langle \mu lm | Y_{l'' m''} | \mu' l' m' \rangle R_{l'' m''}$, the sum to right hand side of Eq. (4.2) reduces essentially to two terms, involving matrix elements:

$$\langle 11 | Y_{30} | 21 \rangle = \frac{1}{4} \sqrt{\frac{7}{15\pi}}, \quad \langle 11 | Y_{32} | 2, -1 \rangle = \frac{1}{\sqrt{14\pi}}.$$

Substituting, together with Eq. (4.3), into (4.2) and then into Eqs. (A 7-A 8), we finally obtain:

$$\frac{U_1^{drift}}{\alpha R_0} = \sqrt{\frac{5}{21\pi}} Im[\tilde{R}_{32}], \quad \frac{U_2^{drift}}{\alpha R_0} = \sqrt{\frac{5}{21\pi}} \left(\frac{7}{4} \sqrt{\frac{2}{15}} \tilde{R}_{30} + Re[\tilde{R}_{32}] \right). \quad (4.4)$$

A similar coupling between the $l = 2$ (or $l = 3$) harmonics in a shear flow and $l = 3$ (or $l = 2$) harmonics in the internal properties of a droplet immersed in the flow, has been shown in Hanna & Vlahovska (2010) to induce transverse migration of the droplet.

From $Y_{30} \propto \cos\theta(5\cos^2\theta - 3)$ and $Y_{32} \propto E^{2i\phi} \sin^2\theta \cos\theta$, we see that a tank-treading vesicle drifting to positive x_2 will need to have a shape, whose section in the shear plane $x_2 x_3$ (for $\alpha > 0$) is an egg with the tip at $x_3 > 0$. The geometrical mechanism for drift along x_2 is illustrated in Fig. 2 and parallels what is obtained in the case of the discrete swimmer discussed in Olla (2010). Drift to positive x_1 will require, on the other hand a shape whose section in the $x_1 x_2$ plane is an ellipse with the long axis at $\phi = \pi/4$ with respect to x_1 . A discrete version of a passive swimmer undergoing such a kind of chiral migration has been illustrated in Watari & Larson (2009). In both Olla (2010) and Watari & Larson (2009), the drift was generated in an ensemble of connected spheres rotating in a shear flow, imposing a configuration that was on the average asymmetric in the laboratory reference frame.

We can imagine at this point a hypothetical microswimmer, whose structure is that of a vesicle, with full control of the mechanical properties of its membrane, and ask what modification of κ would be required to achieve the drift behaviors described in Eq. (4.4).

From Eq. (4.4), we see that the drift is maximized if all the excess area is stored in the deformation components $\tilde{R}_{3, \pm 2}$. In order for $\tilde{R}_{2, \pm 1} = 0$, we need that the forcing from the strain components of $\bar{\mathbf{u}}$ in Eq. (3.14), be canceled by the contribution by membrane inhomogeneity. From Eq. (3.15):

$$\tilde{\kappa}_{2, \pm 1} = \frac{i}{4} \sqrt{\frac{10\pi}{3}} Ca, \quad (4.5)$$

The $l = 3$ components of $\tilde{\kappa}$ are obtained imposing in Eq. (3.14) the tank-treading condi-

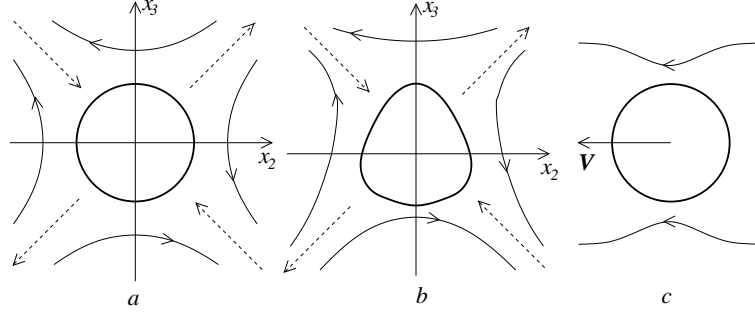


FIGURE 2. Velocity perturbation ($\hat{\mathbf{u}}$ field) around particles in a viscous fluid. (a): a sphere suspended in the shear flow $\bar{\mathbf{u}} = \alpha x_2 \hat{\mathbf{x}}_3$ ($\alpha > 0$; dashed arrows indicate the strain component of $\bar{\mathbf{u}}$); (b): a tank-treading vesicle suspended in the same flow, shaped to drift towards $x_2 > 0$ [see Eq. (4.4)]; (c): a sphere pulled with velocity \mathbf{V} to the left. In case (a), $\hat{u}_2(x_3) = -\hat{u}_2(-x_3)$. In case (b), $\hat{u}_2(x_3) \neq -\hat{u}_2(-x_3)$, and $\hat{u}_2(x_3)$ has an even component which can be shown to have the same sign as the corresponding one in the velocity dipole in (c). In both cases (b) and (c), the net effect is a hydrodynamic force pushing the particle to the right.

tion $\partial \tilde{R}_{3,\pm 2} / \partial \tilde{t} = 0$, together with $\tilde{R}_{3m} = 0$ for $m \neq \pm 2$. Using Eqs. (3.11) and (3.13):

$$\begin{aligned} \tilde{\kappa}_{3,\pm 3} &= -\frac{19\sqrt{6}}{240} \text{iCa} \lambda \tilde{R}_{3,\pm 2}, & \tilde{\kappa}_{3,\pm 1} &= -\frac{19\sqrt{10}}{240} \text{iCa} \lambda \tilde{R}_{3,\pm 2}, \\ \tilde{\kappa}_{3,\pm 2} &= -10(12 + T^{glo}) \tilde{R}_{3,\pm 2}. \end{aligned} \quad (4.6)$$

We see from the third in Eq. (4.6) that the component $\tilde{\kappa}_{3,\pm 2}$ depends on tension T^{glo} , which remains undetermined. A lower bound for the amplitude $|\tilde{\kappa}_{3,\pm 2}|^2$ can be obtained requiring stability of the configuration, i.e. $B_l > 0$, for which it is sufficient that $B_2 > 0$, i.e. $T^{glo} > -6$. From Eq. (2.3), we find therefore:

$$|\tilde{\kappa}_{32}|^2 > (9/5)\epsilon, \quad (4.7)$$

and the arbitrariness of $\tilde{\kappa}_{32}$ reflects the independence of the two expansion parameters of the theory $\epsilon^{1/2}$ and $\tilde{\kappa}$.

5. A vesicle that “swims” in response to concentration gradients

A microswimmer, such as the one described in the previous section, would probably require a sophisticated control system to achieve the bending rigidity modifications described in Eqs. (4.6-4.7). One may ask whether a simpler design is possible, in which the membrane reacts directly to the external environment, without the need of an internal control system.

We are going to describe such a design, in which the vesicle is able to migrate up (or down) a concentration gradient in the shear plane, through softening (or stiffening) of the membrane, in response to a local property of the fluid, such as e.g. the presence of a chemical substance, a temperature inhomogeneity, or a light intensity gradient. A key ingredient will appear to be the presence of a delay in the membrane response to the external environment.

Let us assume that the response of a membrane element in our vesicle, to a concentration field Θ , be described by a linear relaxation equation in the form:

$$(\partial_t + \mathbf{U} \cdot \nabla_{\mathbf{t}} + \gamma) \tilde{\kappa} = \beta \Theta, \quad (5.1)$$

where γ and β could be in general isotropic operators. Equation (5.1) could be seen as

the result, say, of a process of absorption or chemical reaction with the environment (the field Θ may describe e.g. an absorption flux from the bulk, β would be an absorption constant and $\gamma\kappa \propto -\nabla_{\mathbf{t}}^2\kappa$ may account for surface diffusion effects). The flow on the tank-treading membrane is accounted for by the advection term $\mathbf{U} \cdot \nabla_{\mathbf{t}}\tilde{\kappa}$. In stationary conditions, the time derivative will drop off Eq. (5.1).

Let us assume the presence of a concentration gradient along x_2 , so that, on the membrane: $\Theta = \Theta(\mathbf{R}) = \Theta_0 + \Theta'R(\theta, \phi) \sin\theta \sin\phi$. (We assume that the diffusive current responsible for the gradient in Θ is much larger than its advective counterpart $\sim \alpha\Theta'R$, generated by the flow perturbation due to the vesicle). The effect of the constant part Θ_0 is an isotropic contribution to $\tilde{\kappa}$ that could be reabsorbed in a renormalization of κ_0 . To determine the anisotropic part, we expand Eq. (5.1) perturbatively in ϵ :

$$\begin{aligned} (\mathbf{U}^{(0)} \cdot \nabla_{\mathbf{t}} + \gamma)\tilde{\kappa}^{(1)} &= \Theta'R_0\beta \sin\theta \sin\phi, \\ (\mathbf{U}^{(0)} \cdot \nabla_{\mathbf{t}} + \gamma)\tilde{\kappa}^{(2)} &= \Theta'R_0\beta\tilde{R}^{(1)} \sin\theta \sin\phi - \mathbf{U}^{(1)} \cdot \nabla_{\mathbf{t}}\tilde{\kappa}^{(1)}, \end{aligned} \quad (5.2)$$

and so on to higher orders.

Let us focus on the regime in which the relaxation time scale for the membrane properties is much longer than that of the hydrodynamics, that is α^{-1} . In this regime, a membrane will soften (or stiffen) while cruising at $x_2 > 0$, and start stiffening (or softening) when crossing to $x_2 < 0$. In the velocity field described in Eq. (3.1), therefore, our vesicle will present a softer (stiffer) side to $x_3 > 0$, and we would expect an egg shape with tip pointing at $x_3 > 0$ (at $x_3 < 0$). From Eq. (4.4), this would correspond to drift to positive (negative) x_2 . Unfortunately, a linear theory, based only on the first of Eq. (5.2), turns out to be insufficient to account for this effect.

Proceeding as before, we expand Eq. (5.2) in spherical harmonics. The lowest order contribution to advection reads $\mathbf{U}^{(0)} \cdot \nabla_{\mathbf{t}} = \tilde{\mathbf{u}}_{r=R_0}^{rot} \cdot \nabla$; using Eq. (3.12), the first of Eq. (5.2) becomes:

$$\alpha \sum_{m'} \Omega_{lmm'} \tilde{\kappa}_{lm'}^{(1)} + \gamma_l \tilde{\kappa}_{lm}^{(1)} = \beta_l \Theta' R_0 \langle lm | \sin\theta \sin\phi \rangle, \quad (5.3)$$

where now γ_l and β_l are numbers. We see immediately that $\tilde{\kappa}^{(1)}$ is a superposition of $l = 1$ harmonics, which do not contribute, to lowest order in ϵ , to the vesicle dynamics [see Eqs. (3.10,3.11,3.14)]. Thus, to lowest order in $\tilde{\kappa}$, the shape of a vesicle in the shear flow of Eq. (3.1) will be the same as in the case of a homogeneous membrane: an ellipsoid with the long axis between the stretching direction of the flow and the x_3 axis.

At this point, two strategies are possible: one is to replace Eq. (5.1) by a nonlinear model equation; the other is to take into account higher order terms in ϵ in the vesicle response to Θ . Now, an equation like (5.1) describes the response of the membrane to the small variations of Θ that occur on the scale of the vesicle. The physical meaning of a nonlinear version of such equation remains therefore unclear. On the other hand, the higher order terms in the response to Θ , could provide qualitative information on the behavior of strongly non-spherical vesicles. This suggests us to opt for the second strategy, and to focus on the higher order contributions to the membrane response.

We must consider the secondary deformations induced by $\tilde{\kappa}^{(2)}$, and by those non-linear contributions to the $\tilde{\kappa}$ -dependent part of the force exerted by the membrane on the fluid, that were disregarded in Eqs. (2.11) and (2.12). Writing in explicit form:

$$\mathbf{f}^{in} = \mathbf{f}^{in,L} + \mathbf{f}^{in,N}, \quad (5.4)$$

with $\mathbf{f}^{in,L}$ identifying the contribution by $\tilde{\kappa}^{(2)}$, $\mathbf{f}^{in,N}$ accounting for the nonlinear part of the force.

Notice that the force terms in Eq. (5.4) are $O(\tilde{\kappa}\epsilon^{1/2})$. To the same order of accuracy,

also $O(\epsilon)$ terms should be taken into account; one example are the corrections from approximating $R = R_0$ in the Dirac deltas entering \mathbf{f}^B and \mathbf{f}^T [see Eqs. (2.11) and (2.12)]. However, from symmetry of the flow, terms that do not involve $\tilde{\kappa}$ are superpositions of even l harmonics, while drift is produced by $l = 3$ harmonics [see Eq. (4.4)]. Such $O(\epsilon)$ contributions to the force can thus be disregarded.

5.1. Higher order contributions to the bending rigidity

Let us consider first the contribution to the membrane force from $\tilde{\kappa}^{(2)}$, i.e. the term $\mathbf{f}^{in,L}$ in Eq. (5.4). First, however, we have to evaluate the components $\tilde{\kappa}_{lm}^{(1)}$. From $\langle 1, \pm 1 | \sin \theta \sin \phi \rangle = i\sqrt{2\pi/3}$, and using Eq. (3.13) in Eq. (5.3), we find, in the limit $\gamma_1/\alpha \rightarrow 0$:

$$\tilde{\kappa}_{lm}^{(1)} = 4\sqrt{\frac{\pi}{3}}\hat{\kappa}\delta_{l1}\delta_{m0}, \quad \hat{\kappa} = \frac{\beta_l R_0 \Theta'}{\alpha}. \quad (5.5)$$

In order to determine $\tilde{\kappa}^{(2)}$, we have to solve the second of Eq. (5.2). From Eqs. (3.8,3.9) and (3.12), we have $\mathbf{U}^{(1)} \cdot \nabla_{\mathbf{t}} = \alpha \sum_{lmm'} \frac{2}{\sqrt{l(l+1)}} \Omega_{lmm'} R_{lm'}^{(1)} \mathbf{Y}_{Elm} \cdot \nabla$. From Eq. (3.15) and the fact that $\tilde{\kappa}^{(1)}$ has only $l = 1$ components, $R^{(1)}$ will be a superposition of $l = 2$ components. Substituting into the second of Eq. (5.2), passing to spherical harmonics, and using Eq. (5.5), we obtain therefore:

$$\begin{aligned} \tilde{\gamma}_l \tilde{\kappa}_{lm}^{(2)} + \text{Ca} \lambda \sum_{m'} \Omega_{lmm'} \tilde{\kappa}_{lm'}^{(2)} &= \hat{\kappa} \left[\sum_{m'} \langle lm | Y_{2m'} \sin \theta \sin \phi \rangle \tilde{R}_{2m'}^{(1)} \right. \\ &\quad \left. - \frac{8}{3} \sqrt{\frac{2}{3}} \sum_{m'm''} \Omega_{2m'm''} \langle lm | \mathbf{Y}_{Elm'} \cdot \tilde{\nabla} Y_{10} \rangle \tilde{R}_{2m''}^{(1)} \right], \quad (5.6) \end{aligned}$$

where $\tilde{\gamma}_l = \gamma_l/\alpha$.

We shall need only the $l = 3$ components of $\tilde{\kappa}^{(2)}$. Solution of Eq. (5.6), using Eq. (3.13) and the expressions for the matrix elements provided in Appendix C, gives then the result, for $\tilde{\gamma}_3 \rightarrow 0$:

$$\begin{aligned} \tilde{\kappa}_{30}^{(2)} &= \frac{2\hat{\kappa}}{3\sqrt{35}} \left(11\tilde{R}_{20}^{(1)} + 2\sqrt{\frac{2}{3}}\tilde{R}_{22}^{(1)} \right), \\ \tilde{\kappa}_{31}^{(2)} &= \sqrt{\frac{10}{7}}\hat{\kappa}\tilde{R}_{21}^{(1)}, \quad \tilde{\kappa}_{32}^{(2)} = \frac{2\hat{\kappa}}{\sqrt{7}}\tilde{R}_{22}^{(1)}, \quad \tilde{\kappa}_{33}^{(2)} = -\frac{\hat{\kappa}}{3}\sqrt{\frac{2}{21}}\tilde{R}_{21}^{(1)}. \quad (5.7) \end{aligned}$$

The contribution to the bending force is in the same form as Eq. (2.11):

$$\mathbf{f}^{B,in,L} = -\frac{2\kappa_0}{R_0^3} \sum_{lm} \tilde{\kappa}_{lm}^{(2)} [l(l+1)\mathbf{Y}_{Slm} - \sqrt{l(l+1)}\mathbf{Y}_{Elm}] \delta(r - R_0).$$

To this, we must add a tension force contribution $\mathbf{f}^{T,in,L}$, whose effect, as in the derivation of Eq. (3.10), is to cancel the tangential part of $\mathbf{f}^{B,in,L}$. Using Eq. (2.12), we obtain

$$f_{Slm}^{in,L} = -\frac{2\kappa_0}{R_0^3} (l^2 + l - 2) \tilde{\kappa}_{lm}^{(2)} \delta(r - R_0), \quad (5.8)$$

which will lead to a correction term $D_l \tilde{\kappa}_{lm}^{(2)}$ in Eqs. (3.10) and (3.14).

5.2. Nonlinear corrections in the bending force

To lowest order in \tilde{R} , the contribution to force by the $l = 1$ components in $\tilde{\kappa}$ is identically zero. We must consider terms $\propto \tilde{\kappa}\tilde{R}$ in the bending force, which requires keeping terms $\propto \tilde{\kappa}\tilde{R}^2$ in the bending energy. The lowest order contribution to the bending energy due

to the component $\tilde{\kappa}^{(1)}$ is obtained from Eqs. (2.4,2.9,2.10):

$$\begin{aligned} \mathcal{H}^{B,in,N} = \kappa_0 \int & \left\{ \tilde{\kappa}^{(1)} \left[\tilde{R}^{(1)} \tilde{\nabla}_{\mathbf{t}}^2 \tilde{R}^{(1)} + \frac{1}{2} (\tilde{\nabla}_{\mathbf{t}}^2 \tilde{R}^{(1)})^2 \right] \right. \\ & \left. - \tilde{R}^{(1)} \left[(\partial_\theta \tilde{R}^{(1)}) (\partial_\theta \tilde{\kappa}^{(1)}) + \frac{(\partial_\phi \tilde{R}^{(1)}) (\partial_\phi \tilde{\kappa}^{(1)})}{\sin^2 \theta} \right] \right\} \sin \theta d\theta d\phi. \end{aligned}$$

Using Eq. (2.7), this corresponds to a force density:

$$\begin{aligned} \mathbf{f}^{B,in,N} = \frac{\kappa_0}{R_0^3} & \left\{ [2\tilde{\kappa}^{(1)} (1 + \tilde{\nabla}_{\mathbf{t}}^2) \tilde{\nabla}_{\mathbf{t}}^2 \tilde{R}^{(1)} + (\tilde{\nabla}_{\mathbf{t}}^2 \tilde{\kappa}^{(1)}) (\tilde{\nabla}_{\mathbf{t}}^2 \tilde{R}^{(1)}) \right. \\ & \left. + \frac{1}{2} \tilde{R}^{(1)} \tilde{\nabla}_{\mathbf{t}}^4 \tilde{\kappa}^{(1)} \right] \mathbf{e}_r + 2(\tilde{\nabla}_{\mathbf{t}}^2 \tilde{R}^{(1)}) \tilde{\nabla}_{\mathbf{t}} \tilde{\kappa}^{(1)} \left. \right\} \delta(r - R_0). \end{aligned} \quad (5.9)$$

As with the other force terms, a tension contribution must be added, that cancels the tangential component in Eq. (5.9) and produces a correction to the normal part, with $f_{Slm}^{T,in,N} = \frac{\sqrt{l(l+1)}}{2} f_{Elm}^{T,in,N}$ [see Eq. (2.12)]. In terms of vector spherical harmonics, the resulting total force will read, using Eq. (5.5):

$$\begin{aligned} f_{Slm}^{in,N} = -\frac{8\kappa_0}{R_0^3} & \sqrt{\frac{\pi}{3}} \left\{ 37 \langle lm | Y_{10} | 2m \rangle \right. \\ & \left. - \frac{12}{\sqrt{l(l+1)}} \langle Elm | \tilde{\nabla}_{\mathbf{t}} Y_{10} | 2m \rangle \right\} \hat{\kappa} \tilde{R}_{2m}^{(1)} \delta(r - R_0), \end{aligned} \quad (5.10)$$

and again, to determine the drift, only the $l = 3$ force components will be required.

5.3. Contribution to drift

The $l = 3$ components of the total membrane force are obtained putting together Eqs. (5.7,5.8,5.10). Substituting into Eq. (3.14) and using the expression for the matrix elements provided in Appendix C, leads to the following equation for the $l = 3$ component of the secondary vesicle deformation:

$$\lambda \text{Ca} A_3 \sum_{m'} \Omega_{3mm'} \tilde{R}_{3m'}^{(2)} + B_3 \tilde{R}_{3m}^{(2)} = \hat{\kappa} \sum_{m'} E_{3mm'} R_{2m'}^{(1)} \quad (5.11)$$

where the only non-zero entries of the matrix $E_{3mm'}$ are:

$$\begin{aligned} E_{300} &= -\frac{1628}{3\sqrt{35}}, & E_{302} &= -\frac{80}{3} \sqrt{\frac{6}{35}}, \\ E_{311} &= -364 \sqrt{\frac{2}{35}}, & E_{322} &= -\frac{172}{\sqrt{7}}, & E_{331} &= -\frac{20}{3} \sqrt{\frac{2}{21}}. \end{aligned} \quad (5.12)$$

The lowest order components $\tilde{R}_{lm}^{(1)}$ describe the shape of a vesicle with homogeneous membrane, in the flow (3.1). The behavior in a viscous shear flow of a vesicle with such characteristics is well understood (Noguchi & Gompper 2007; Lebedev *et Al.* 2007; Farutin *et Al.* 2010); the features relevant to the present analysis are summarized in Appendix B. We have:

$$\tilde{R}_{22}^{(1)} = \frac{1}{\sqrt{6}} \tilde{R}_{20}^{(1)} = \frac{1}{4} \frac{\lambda}{\lambda_{cr}} \epsilon^{1/2}, \quad \tilde{R}_{21}^{(1)} = \frac{i}{2} \sqrt{1 - (\lambda/\lambda_{cr})^2} \epsilon^{1/2}, \quad (5.13)$$

where

$$\lambda_{cr} = 4 \sqrt{\frac{10\pi}{3\epsilon}} \quad (5.14)$$

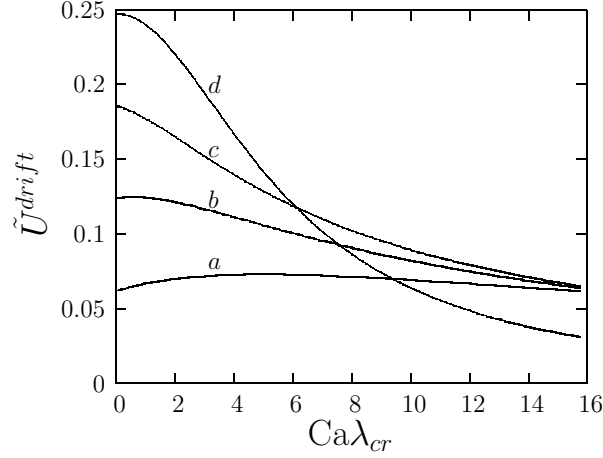


FIGURE 3. Profiles of the normalized drift velocity $\tilde{U}^{drift} = -U_2^{drift}/(\alpha R_0 \hat{\kappa} \epsilon^{1/2})$, in function of $\text{Ca} \lambda_{cr}$ for different values of λ/λ_{cr} . In the four cases: (a): $\lambda/\lambda_{cr} = 0.25$; (b): $\lambda/\lambda_{cr} = 0.5$; (c): $\lambda/\lambda_{cr} = 0.75$; (d): $\lambda/\lambda_{cr} = 1$. The drift vanishes in the limit $\lambda/\lambda_{cr} \rightarrow 0$.

is the maximum viscosity contrast for which tank-treading is possible. In the small Ca regime considered [see Eq. (3.6)], for $\lambda > \lambda_{cr}$, the vesicle will make direct transition to a tumbling regime, in which the vesicle rotates in the shear plane as a rigid object (Farutin *et Al.* 2010).

The membrane tension, entering the relaxation coefficient B_3 in Eq. (5.11) [see the second of Eq. (3.11)], is determined, to lowest order in ϵ and $\hat{\kappa}$, by the shape dynamics accounted for by Eq. (5.13):

$$T^{glo} = -6 + \frac{\lambda_{cr} \text{Ca}}{4} \sqrt{1 - (\lambda/\lambda_{cr})^2}. \quad (5.15)$$

To the order considered in Eq. (5.11), the contribution to tension by the secondary deformation $\tilde{R}^{(2)}$ is disregarded.

Using Eqs. (5.12-5.15), Eq. (5.11) can be solved in terms of the dimensionless parameters $\hat{\kappa}$, λCa and λ_{cr} (or ϵ). From here, substituting into Eq. (4.4), the drift velocity can be expressed in the form

$$U_2^{drift} = -\tilde{U}^{drift}(\lambda/\lambda_{cr}, \text{Ca} \lambda_{cr}) \hat{\kappa} \epsilon^{1/2} \alpha R_0.$$

Notice that the arguments of \tilde{U}^{drift} , given the scaling in Eq. (3.6), are not singular in the limit $\epsilon \rightarrow 0$. The profile of the normalized drift velocity \tilde{U}^{drift} is illustrated in Fig. 3; we see that the maximum is attained for $\lambda/\lambda_{cr} = 1$ and $\text{Ca} \lambda_{cr} = 0$, in which case

$$U_2^{drift} = -\frac{4279}{37800} \sqrt{\frac{15}{\pi}} \hat{\kappa} \epsilon^{1/2} \alpha R_0 \simeq -0.25 \hat{\kappa} \epsilon^{1/2} \alpha R_0. \quad (5.16)$$

As expected, softening of the membrane in regions of higher Θ , (which implies $\hat{\kappa} < 0$), will lead to an up-gradient drift of the vesicle.

The increase of \tilde{U}^{drift} as $\lambda/\lambda_{cr} \rightarrow 1$ and $\text{Ca} \lambda_{cr} \rightarrow 0$, shown in Fig. 3, is associated with a complex pattern of vesicle deformations. Passing from $\lambda = \lambda_{cr}$ to $\lambda = 0$ for $\text{Ca} \lambda_{cr}$ fixed, the long axis of the ellipsoid described by the components $R_{2m}^{(1)}$ will shift from alignment with the flow, to an orientation at $\pi/4$ with respect to it. At the same time, the components $R_{3m}^{(2)}$ with $m = 0, 2$, that are associated with drift, will go to zero in the limit. [This is consequence of the fact that the matrix elements E_{lmm} , as described in

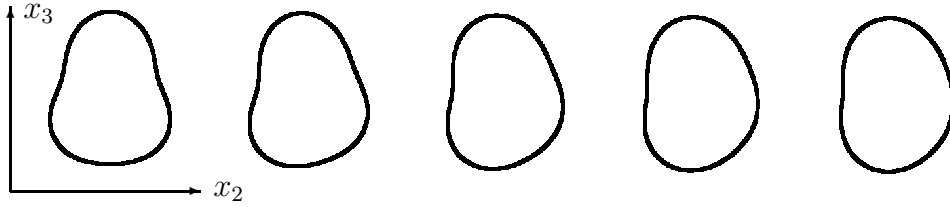


FIGURE 4. Sketch of the vesicle orientation in the x_2x_3 plane for $\lambda/\lambda_{cr} = 1$ and different values of $Ca \lambda_{cr}$. From left to right: $Ca \lambda_{cr} = 0, 3.2, 6.3, 9.5, 12.6$. In all cases, $\hat{\kappa} < 0$, corresponding to drift to $x_2 > 0$. The shapes have been drawn starting from Eqs. (2.1,B2) and (5.11), greatly exaggerating the amplitude of the components $R_{2m}^{(1)}$ and $R_{3m}^{(2)}$.

Eq. (5.12), do not mix even and odd m components, and that the rotation term in Eq. (5.11) vanishes in the limit. In other words, the fore-aft axis of the vesicle, associated with $R^{(2)}$, and the long ellipsoid axis, align at $\pi/4$ with respect to the flow].

For the same reason, the fore-aft and the long ellipsoid axis will align for $Ca \lambda_{cr} \rightarrow 0$, and λ/λ_{cr} fixed. At $\lambda = \lambda_{cr}$, this will occur along the flow direction, which maximizes \tilde{U}^{migr} (in fact, $R_{3m}^{(2)}$ has only $m = 0, 2$ components). The shift in the vesicle orientation, occurring in the process, is illustrated in Fig. 4.

6. Conclusion

A microswimmer could in principle exploit velocity gradients in the suspending fluid as a means for propulsion. We have seen that a vesicle could obtain this result by control over the bending rigidity of its membrane. The additional stresses induced in the membrane by its own inhomogeneities (Goulian *et Al.* 1993) could be exploited to counteract the effect of the external flow and to allow vesicle shapes and orientations that would otherwise be forbidden.

In the case of an unbounded linear shear, a vesicle with such capabilities could migrate transverse to the flow, both in the shear plane and perpendicular to it. Propulsion is achieved through modulation of tank-treading by inhomogeneity of the membrane properties, which results in a constant fore-aft asymmetric shape for the vesicle (an egg-shape with tip along the flow, in case of in-plane drift) and a dipole component in velocity perturbation around it, associated with the presence of a transverse force.

These calculations can be easily extended to the case of a shear flow bounded by a wall, thus allowing to consider regimes in which a tank-treading vesicle could be made to drift towards a wall, rather than away from it, as occurring normally with an homogeneous membrane (Abkarian *et Al.* 2002).

We have shown that such migration behaviors (at least, those confined to the shear plane) could be achieved simply by a stiffening (or softening) of the membrane, in response to variations of some local fluid properties, e.g. a chemical concentration. With an appropriate choice of parameters in the membrane response, a vesicle could be made to migrate automatically, up or down a concentration gradient in the shear plane, without the need of complicated control systems.

The results discussed have been obtained through a perturbative calculation in the case of a quasi-spherical vesicle. In this regime, the migration velocity is smaller than the velocity scale αR_0 (the velocity difference in the shear flow at the vesicle scale), by a factor $\tilde{\kappa}\epsilon^{1/2}$, with ϵ the normalized excess area and $\tilde{\kappa}$ the degree of inhomogeneity of the bending energy [see Eqs. (2.3) and (2.6)]. However, as the mechanisms for stress generation by membrane inhomogeneity, and for migration by asymmetry of the vesicle

shape, are essentially geometric, the same behaviors are expected to hold also for strongly non-spherical vesicles and strong inhomogeneity in the bending rigidity.

In the present analysis, no attention has been given to the problem of the material that could be utilized to synthesize a membrane with the properties described in Eqs. (4.6,4.7), or in Eq. (5.1). In principle, the required local modifications of the membrane could be achieved by some sort of absorption process or chemical process with the bulk, in analogy with what is done in experiments on the Marangoni effect (Kitahata *et Al.* 2002) and osmophoresis (Nardi *et Al.* 1999). It remains to be determined, however, which material could satisfy the requirements imposed by Eq. (5.1), in particular, slow relaxation of membrane properties, compared to hydrodynamic time-scales. At the present stage, therefore, as in the case of most microswimmer designs, also the present vesicle-based one remains at the level of a purely theoretical model.

It must be said that the adoption of a vesicle based microswimmer design, rather than a microcapsule based one, has been motivated purely by simplicity considerations on the constitutive law for the membrane. After all, tank-treading behaviors, similar to those of vesicles, are observed also in the case of microcapsules (Barthes-Biesel 1980; Pozrikidis 2003; Skotheim & Secomb 2007). This could open additional possibilities as regards the issue of practical realization. An interesting question is whether a microswimmer design, utilizing an elastic, rather than fluid membrane, would be more effective in converting fluid stresses into migration.

The author wishes to thank Alexander Farutin and Chaoqui Misbah for interesting and helpful discussion.

Appendix A. Lamb representation

The Stokes equation for an incompressible fluid are

$$\eta \nabla^2 \mathbf{v} = \nabla P, \quad \nabla \cdot \mathbf{v} = 0, \quad (\text{A } 1)$$

where P is the pressure. This equation can be solved in the basis of Eq. (2.2), with boundary conditions $\mathbf{v} = \mathbf{V}$ imposed on a surface $r = R_0$; the result is the so called Lamb representation of the Stokes equation (Happel & Brenner 1973). The solutions for $r < R_0$ and $r > R_0$ read respectively:

$$\begin{aligned} v_{Slm}^{in} &= \frac{1}{2} \left[(l+3 - (l+1)y^2) V_{Slm} + \sqrt{l(l+1)}(y^2 - 1) V_{Elm} \right] y^{l-1} \\ v_{Elm}^{in} &= \frac{1}{2} \left[(l+3) \sqrt{\frac{l+1}{l}} (1 - y^2) V_{Slm} + (-(l+1) + (l+3)y^2) V_{Elm} \right] y^{l-1} \\ v_{Mlm}^{in} &= V_{Mlm} y^l. \end{aligned} \quad (\text{A } 2)$$

and

$$\begin{aligned} v_{Slm}^{out} &= \frac{1}{2} \left[(l + (2-l)y^{-2}) V_{Slm} + \sqrt{l(l+1)}(l - y^{-2}) V_{Elm} \right] y^{-l} \\ v_{Elm}^{out} &= \frac{1}{2} \left[(2-l) \sqrt{\frac{l}{l+1}} (1 - y^{-2}) V_{Slm} + (2-l + ly^{-2}) V_{Elm} \right] y^{-l}, \\ v_{Mlm}^{out} &= V_{Mlm} y^{-1-l}, \end{aligned} \quad (\text{A } 3)$$

where $y = r/R_0$.

The shear flow $\hat{\mathbf{u}} = \alpha x_2 \hat{\mathbf{x}}_3$ and \mathbf{u} , that is the flow inside the vesicle, are both in the form of \mathbf{v}^{in} , while the perturbation $\hat{\mathbf{u}}$ is in the form of \mathbf{v}^{out} . The lowest order solutions $\hat{\mathbf{u}}^{(0)}$ and $\mathbf{u}^{(0)}$ are given by Eqs. (A 3) and (A 2) with $\mathbf{V} = \hat{\mathbf{U}}^{(0)}$ and $\mathbf{V} = \mathbf{U}^{(0)}$. To higher order in \hat{R} , different harmonics in $\hat{\mathbf{U}}$, \mathbf{U} and $\hat{\mathbf{u}}$, \mathbf{u} get mixed due to deviation from spherical shape.

The vector spherical components on the surface $r = R_0$ for the shear flow $\bar{\mathbf{u}}$ are obtained from Eq. (A 2):

$$\frac{\bar{U}_{S2,\pm 1}^{(0)}}{\alpha R_0} = i\sqrt{\frac{2\pi}{15}}, \quad \frac{\bar{U}_{E2,\pm 1}^{(0)}}{\alpha R_0} = i\sqrt{\frac{\pi}{5}} \quad \text{and} \quad \frac{\bar{U}_{M1,\pm 1}^{(0)}}{\alpha R_0} = \pm\sqrt{\frac{\pi}{3}}. \quad (\text{A } 4)$$

It is easy to see that $U_{M1,\pm 1}^{(0)}$ is responsible for the vorticity part of the velocity $\bar{\mathbf{u}}^{rot} = \frac{1}{2}\alpha(x_2\hat{\mathbf{x}}_3 - x_3\hat{\mathbf{x}}_2)$.

The force density on the surface $r = R_0$, produced by the internal field in Eq. (A 2) will read, in dimensionless form:

$$\begin{aligned} g_{Slm}(\mathbf{V}) &= \frac{1}{\alpha R_0} \left[-\frac{2l^2+l+3}{l} V_{Slm} + 3\sqrt{\frac{l+1}{l}} V_{Elm} \right], \\ g_{Elm}(\mathbf{V}) &= \frac{1}{\alpha R_0} \left[3\sqrt{\frac{l+1}{l}} V_{Slm} - (2l+1)V_{Elm} \right], \\ g_{Mlm}(\mathbf{V}) &= -\frac{(l-1)}{\alpha R_0} V_{Mlm} \end{aligned} \quad (\text{A } 5)$$

and the one from the external field, Eq. (A 3):

$$\begin{aligned} \hat{g}_{Slm}(\mathbf{V}) &= -\frac{1}{\alpha R_0} \left[\frac{2l^2+3l+4}{l+1} V_{Slm} + 3\sqrt{\frac{l}{l+1}} V_{Elm} \right], \\ \hat{g}_{Elm}(\mathbf{V}) &= \frac{1}{\alpha R_0} \left[3\sqrt{\frac{l}{l+1}} V_{Slm} - (2l+1)V_{Elm} \right], \\ \hat{g}_{Mlm}(\mathbf{V}) &= -\frac{(l+2)}{\alpha R_0} V_{Mlm}. \end{aligned} \quad (\text{A } 6)$$

The total hydrodynamic force \mathbf{F} on the vesicle is obtained from the $\mu = S, E, l = 1$ components of the outer Lamb solution (A 3) $\hat{\mathbf{u}}$. In particular, for the force components along $\hat{\mathbf{x}}_{1,2}$:

$$\begin{aligned} F_1 &= 2\sqrt{6\pi}\eta_{ext}R_0 \operatorname{Re}(\hat{U}_{S11}^{(1)} + \sqrt{2}\hat{U}_{E11}^{(1)}), \\ F_2 &= -2\sqrt{6\pi}\eta_{ext}R_0 \operatorname{Im}(\hat{U}_{S11}^{(1)} + \sqrt{2}\hat{U}_{E11}^{(1)}), \end{aligned} \quad (\text{A } 7)$$

where we have used the fact that, from Eqs. (3.4) and (A 4): $\hat{U}_{\mu 11}^{(0)} = 0$ for $\mu = S, E$. In the absence of external forces, this is cancelled by the drag force $-D_0\mathbf{U}^{drift}$ on a vesicle migrating with velocity \mathbf{U}^{drift} , where, to lowest order in ϵ , D_0 is the Stokes drag by a spherical vesicle. Now, a spherical vesicle with an inextensible membrane will behave with respect to the fluid as a rigid object [except for solenoidal flow components \mathbf{U}_{Mlm} on the surface, that do not couple with \mathbf{U}^{drift} ; see Eqs. (3.8) and (3.9)]. Hence, D_0 is the drag coefficient of a rigid sphere. The drift velocity of the vesicle will be therefore, to lowest order in ϵ :

$$\mathbf{U}^{drift} = \mathbf{F}/D_0, \quad (\text{A } 8)$$

where $D_0 = 6\pi\eta_{ext}R_0$ is the Stokes drag for a rigid sphere of radius R_0 .

Appendix B. Dynamics of the homogeneous membrane in a shear flow

Assuming a tank-treading regime, the shape of a vesicle in the shear flow (3.1) is obtained from Eq. (3.14) setting the time derivative equal to zero. Using Eqs. (3.11,3.13) and (3.15), and setting to zero the inhomogeneous contribution $D_l\tilde{\kappa}_{lm}$:

$$\begin{aligned} \frac{i\text{Ca}\Lambda}{2}\tilde{R}_{21}^{(1)} + B_2\tilde{R}_{22}^{(1)} &= 0, \\ i\text{Ca}\Lambda \left[\frac{\tilde{R}_{22}^{(1)}}{2} + \frac{\sqrt{6}}{4}\tilde{R}_{20}^{(1)} \right] + B_2\tilde{R}_{21}^{(1)} &= 2i\text{Ca}\sqrt{\frac{10\pi}{3}}, \end{aligned} \quad (\text{B } 1)$$

$$\frac{i\sqrt{6}\text{Ca}\Lambda}{2}\tilde{R}_{21}^{(1)} + B_2\tilde{R}_{20}^{(1)} = 0, \quad \Lambda = A_2\lambda,$$

which gives the result

$$\tilde{R}_{20}^{(1)} = K\text{Ca}\Lambda\sqrt{6}, \quad \tilde{R}_{21}^{(1)} = 2KB_2i, \quad \tilde{R}_{22}^{(1)} = K\text{Ca}\Lambda, \quad (\text{B } 2)$$

where

$$K = \frac{\text{Ca}}{B_2^2 + (\text{Ca}\Lambda)^2} \sqrt{\frac{10\pi}{3}}. \quad (\text{B } 3)$$

Substituting Eqs. (B 2) and (B 3) into the area constrain (2.3), we obtain

$$B_2 = \sqrt{\frac{160\pi\text{Ca}^2}{3\epsilon} - (\text{Ca}\Lambda)^2}, \quad (\text{B } 4)$$

from which we obtain Eq. (5.15). Exploiting the first of Eq. (3.11), we see that tank-treading is possible for

$$\lambda < \lambda_{cr} = \frac{24}{23} \sqrt{\frac{10\pi}{3\epsilon}},$$

that coincides, to leading order in ϵ , with the result in Farutin *et Al.* (2010). Substituting Eq. (B 4) into Eqs. (B 3) and (B 2), we obtain Eq. (5.13).

Appendix C. Matrix elements involving scalar and vector spherical harmonics

We provide below expressions for the matrix elements entering Eqs. (5.5,5.11,5.12).

$$\begin{aligned} \langle 30|Y_{21} \sin \theta \sin \phi \rangle &= i\sqrt{\frac{3}{70}}, & \langle 31|Y_{20} \sin \theta \sin \phi \rangle &= i\sqrt{\frac{3}{35}}, \\ \langle 31|Y_{22} \sin \theta \sin \phi \rangle &= \frac{i}{\sqrt{70}}, & \langle 32|Y_{21} \sin \theta \sin \phi \rangle &= \frac{i}{\sqrt{7}}, \\ \langle 33|Y_{22} \sin \theta \sin \phi \rangle &= i\sqrt{\frac{3}{14}}, & \langle 30|\mathbf{Y}_{E20} \cdot \tilde{\nabla} Y_{10} \rangle &= -3\sqrt{\frac{3}{35\pi}}, \\ \langle 31|\mathbf{Y}_{E21} \cdot \tilde{\nabla} Y_{10} \rangle &= -2\sqrt{\frac{6}{35\pi}}, & \langle 32|\mathbf{Y}_{E22} \cdot \tilde{\nabla} Y_{10} \rangle &= -\sqrt{\frac{3}{7\pi}}, \\ \langle 30|Y_{10}|20 \rangle &= \frac{3}{2}\sqrt{\frac{3}{35\pi}}, & \langle 31|Y_{10}|21 \rangle &= \sqrt{\frac{6}{35\pi}}, \\ \langle 32|Y_{10}|22 \rangle &= \frac{1}{2}\sqrt{\frac{3}{7\pi}}, & \langle E30|\tilde{\nabla} Y_{10}|20 \rangle &= \frac{3}{\sqrt{35\pi}}, \\ \langle E31|\tilde{\nabla} Y_{10}|21 \rangle &= 2\sqrt{\frac{2}{35\pi}}, & \langle E32|\tilde{\nabla} Y_{10}|22 \rangle &= \frac{1}{\sqrt{7\pi}}. \end{aligned}$$

REFERENCES

- ABKARIAN, M., LARTIGUE, C. & VIALLAT, A. 2002 Tank-treading and unbinding of deformable vesicles in shear flow: determination of the lift force *Phys. Rev. Lett.* **88**, 068103
- AVRON, J.E., KENNETH, O. & OAKNIN, D.K. 2005 Pushmepullyou: an efficient microswimmer *New J. Phys.* **7** 234

- BARTHES-BIESEL, D. 1980 Motion of a spherical microcapsule freely suspended in a linear shear flow *J. Fluid Mech.* **100**, 831
- BEHKAM, B. & SITTI, M. 2006 Design Methodology for Biomimetic Propulsion of Miniature Swimming Robots *J. Dyn. Sys., Meas., Control* **128**, 36
- BERG, H.C. 1976 How spirochetes may swim *J. Theor. Biol.* **56**, 269
- BERG, H.C. 2004 *E. coli in motion* Springer
- BLAKE, R.J. 1971 A spherical envelope approach to ciliary propulsion *J. Fluid Mech.* **46**, 199
- BLAKE, R.J. & SLEIGH, M.A. 1974 Mechanics of ciliary locomotion *Biol. Rev. Camb. Phil. Soc.* **49**, 85
- BLUM, J.J. & HINES, M. 1979 Biophysics of flagellar motility *Quarterly Rev. Biophys.* **12**, 103
- CHILDRESS, S. 1981 *Mechanics of swimming and flying* C.U. Press
- COUPIER, G., KAOU, B., PODGORSKI, T. & MISBAH, C. 2008 Noninertial lateral migration of vesicles in bounded Poiseuille flow *Phys. Fluids* **20**, 111702
- DANKER, G., VLAHOVSKA, P.M. & MISBAH, C. 2009 Vesicles in Poiseuille flows *Phys. Rev. Lett.* **102**, 148102
- DREYFUS, R., BAUDRY, J., ROPER, M.L., FERMIGIER, M., STONE, H.A. & BIBETTE, J. 2005 Microscopic artificial swimmers *Nature* **437**, 862
- EHLERS, K.M., SAMUEL, A.D., BERG, H.C. & MONTGOMERY, R. 1996 Do cyanobacteria swim using traveling surface waves? *Proc. Natl. Acad. Sci. USA* **93**, 8340
- FARUTIN, A., BIBEN, T. & MISBAH, C. 2010 Analytical progress in the theory of vesicles under linear flow *Phys. Rev. E* **81**, 061904
- FURTADO, K., POOLEY, C.M. & YEOMANS, J.M. 2008 Lattice Boltzmann study of convective drop motion driven by nonlinear chemical kinetics *Phys. Rev. E* **78**, 046308
- GOLESTANIAN, R., LIVERPOOL, T.D. & AJDARI, A. 2005 Propulsion of a Molecular Machine by Asymmetric Distribution of Reaction Products *Phys. Rev. Lett.* **94**, 220801
- GOLESTANIAN, R. & AJDARI, A. 2008 Analytic results for the three-sphere swimmer a low Reynolds numbers *Phys. Rev. E* **77**, 036308
- GOLESTANIAN, R. & AJDARI, A. 2009 Stochastic low Reynolds number swimmers *J. Phys. Condens. Matter* **21**, 204104
- GOULIAN, M., BRUINSMA, R. & PINCUS, P. (1993) Long-range forces in heterogeneous membranes *Europhys. Lett.* **22**, 145
- HANNA, J.A. & VLAHOVSKA, P.M. 2001 Surfactant-induced migration of a spherical drop in Stokes flow *Phys. Fluids* **22**, 013102
- HAPPEL, J. & BRENNER, H. 1973 *Low Reynolds number hydrodynamics* Kluwer
- ISHIKAWA, T. & PEDLEY, T.J. 2008 Coherent Structures in Monolayers of Swimming Particles *Phys. Rev. Lett.* **100**, 088103
- KITAHATA, H., AIHARA, R., MAGOME, N. & YOSHIKAWA, K. 2002 Convective and periodic motion driven by a chemical wave *J. Chem. Phys.* **116**, 5666
- KRAUS, M., WINTZ, W., SEIFERT, U. & LIPOWSKY, R. 1996 Fluid vesicles in shear flow *Phys. Rev. Lett.* **77**, 3685
- JENKINS, J.T. 1977 The equations of mechanical equilibrium of a model membrane *SIAM (Soc. Ind. Appl. Math.) J. Appl. Math.* **32**, 755
- LAUGA, E. & POWERS, T. 2009 The hydrodynamics of swimming microorganisms *Rep. Prog. Phys.* **72**, 096601
- LEBEDEV, V.V., TURITSYN, K.S. & VERGELES, S.S. 2007 Dynamics of nearly spherical vesicles in an external flow *Phys. Rev. Lett.* **99**, 218101
- LEONI, M., KOTAR, J., BASSETTI, B., CICUTA, P., LAGOMARSINO, M.C. 2009 A basic swimmer at low Reynolds number *Soft Matter* **5**, 472
- LESHANSKY, A.M. & KENNETH, O. 2008 Surface tank-treading propulsion of Purcell's toroidal swimmer *Phys. Fluids* **20**, 063104
- LIGHTHILL, M.J. 1952 On the squirming motion of nearly spherical deformable bodies through liquids at very small Reynolds numbers *Commun. Pure Appl. Math.* **5**, 109
- LIGHTHILL, J. 1957 *Mathematical biofluidynamics* SIAM
- LOBASKIN, V., LOBASKIN, D. & KULIC, I.M. 2008 Brownian dynamics of a microswimmer *Eur. Phys. J. Special Topics* **157**, 149

- NAJAFI, A. & GOLESTANIAN, R. 2004 Simple swimmer at low Reynolds number: Three linked spheres *Phys. Rev. E* **69**, 062901
- NARDI, J., BRUINSMA, R. & SACKMANN, E. 1999 Vesicles as osmotic motors *Phys. Rev. Lett.* **82**, 5168
- NOGUCHI, H. & GOMPPER, G. 2007 Swinging and tumbling of fluid vesicles in shear flow *Phys. Rev. Lett.* **98**, 128103
- OLLA, P. 1997 The lift on a tank-treading ellipsoidal cell in a bounded shear flow *J. Phys. II France* **7**, 1533
- OLLA, P. 2000 The behavior of closed inextensible membranes in linear and quadratic shear flows *Physica A* **278**, 87
- OLLA, P. 2010 Passive swimming in low Reynolds number flows *Phys. Rev. E* **82**, 015302(R)
- PAXTON, W.E., SUNDARARAJAN, S., MALLOUK, T.E. & SEN, A. 2006 Chemical locomotion *Angew. Chem. Int. Ed.* **45**, 5420
- POOLEY, C.M. & BALAZS, A.C. 2007 Producing swimmers by coupling reaction-diffusion equations to a chemically responsive material *Phys. Rev. E* **76**, 016308
- POZRIKIDIS, C. 2003 *Modelling and simulation of capsules and biological cells* Chapman & Hall/CRC
- PURCELL, E.M. 1977 Life at low Reynolds numbers *Am. J. Phys.* **45**, 3
- SEIFERT, U. 1999 Fluid membranes in hydrodynamic flow fields: formalism and an application to fluctuating quasi-spherical vesicles in shear flows *Eur. Phys. J. B* **8**, 405
- SHAPER, A. & WILCZEK, F. 1989 Geometry of self-propulsion at low Reynolds numbers *J. Fluid Mech.* **198**, 557
- SKOTHEIM, J.M. & SECOMB, T.W. 2007 Red blood cells and other non-spherical capsules in shear flow: oscillatory dynamics and the tank-treading to tumbling transition *Phys. Rev. Lett.* **98**, 078301
- STONE, H. A. & SAMUEL, A.D.T. 1996 Propulsion of microorganisms by surface distortions *Phys. Rev. Lett.* **77**, 4102
- SUBRAMANIAN, R.S. & BALASUBRAMANIAM, R. 2001 *The motion of bubbles and drops in reduced gravity* Cambridge
- SUKUMARAN, S. & SEIFERT, U. 2001 Influence of shear flow on vesicles near a wall: a numerical study *Phys. Rev. E* **64**, 011916
- TIERNO, P., GOLESTANIAN, R., PAGONABARRAGA, I. & SAGUÉS, F. 2008 Controlled swimming in confined fluids of magnetically actuated colloidal rotors *Phys. Rev. Lett.* **101**, 218304
- VAND, V. 1948 Viscosity of Solutions and Suspensions. I. Theory *J. Phys. Chem.* **52**, 277
- WATARI, N. & LARSON, R.G. 2009 Shear-induced migration of particles with anisotropic rigidity *Phys. Rev. Lett.* **102**, 246001
- YOUNG, N.O., GOLDSTEIN, J.S. & BLOCK, M.J. 1959 The motion of bubbles in a vertical temperature gradient *J. Fluid Mech.* **6**, 350
- YU, T.S., LAUGA, E. & HOSOI, A.E. 2006 Experimental Investigations of Elastic Tail Propulsion at Low Reynolds Number *Phys. Fluids* **18**, 091701
- ZHONG-CAN, O.-Y. & HELFRICH, W. 1989 Bending energy of vesicle membranes: general expressions of the first, second and third variation of the shape energy and application to spheres and cylinders *Phys. Rev. A* **39**, 5280